Title
P-BAND RADAR MAPPING OF FOREST BIOMASS IN BOREAL FORESTS OF INTERIOR ALASKA

Authors
RIGNOT, E
WAY, JB
WILLIAMS, C
et al.

Publication Date
1994

P-band Radar Mapping of Forest Biomass in Boreal Forests of Interior Alaska

E. Rignot[1], J.B. Way[1], C. Williams[2], L. Viereck[2], J. Yarie[3]

[1] *Jet Propulsion Laboratory, California Institute of Technology, Pasadena CA 91109*

Ph (818) 354-1640; Fax (818) 393-6943

[2] † *Institute of Northern Forestry, U.S. Forest Service, Fairbanks, AK 99775 USA*

[3] • *Department of Forest Science, University of Alaska Fairbanks, Fairbanks, AK 99775 USA*

Abstract

AIRSAR data gathered in winter, spring, and summer over the Bonanza Creek Experimental Forest, near Fairbanks, Alaska are compared to estimates of whole-tree aboveground dry biomass from 21 forest stands and 2 clear-cuts. Using empirical relationships, biomass values are predicted from the radar at various frequencies and polarizations and compared to actual biomass values. Predicted biomass levels are most accurate at P-band. At that frequency, the radar discriminates 7 biomass levels, up to the maximum observable biomass level for these forests, with 18 % error. Within these 7 biomass levels data dispersion is large because of significant inner-stand spatial variations in biomass, interactions of the radar signals with a spatially varying three-dimensional structure of the canopy, as well as uncertainties associated with the estimation of stand biomass from empirical equations. Multiple incidence angle data also reveal that the incidence angle θ_i of the radar illumination affects the retrieval of biomass from the radar data even at HV-polarization when $\theta_i > 50^o$ or $\theta_i < 25^o$. One consequence is that topographic information is required for mapping biomass in areas of moderate topography. Finally, the inversion curve for biomass retrieval varies with season and environmental conditions.

1. Introduction

In undisturbed, even-aged, mono-specie pine plantations in temperate regions with nearly level topography, airborne radar experiments showed radar backscatter is positively correlated with total aboveground dry biomass until it saturates at a level which is higher with increasing radar wavelengths [1-2]. At the same time, modeling and simulation results suggest the effect on radar backscatter of tree structure, vegetation moisture condition and status, as well as the effect of understory condition and topography can be significant and thereby complicate the inference of aboveground biomass from the radar [3-5]. Here, we examine these effects in a natural forest setting, the Bonanza Creek Experimental Forest (BCEF), a Long-Term Ecological Research site (LTER) (64° 45'N, -148°W), near Fairbanks, Alaska.

The vegetation landscape at BCEF is a mosaic of forest, grassland, shrubs, bog and tundra types that have formed primarily as a result of slope, aspect, elevation, parent material and succession after wildfire [6-7]. Presence or absence of permafrost, and solar illumination angle, both correlated with slope and aspect, are dominant factors in the distribution of vegetation types. The forest site includes both upland fire-controlled succession, and floodplain succession forests. Upland forest types vary from highly productive aspen, paper birch and white spruce stands on well-drained, nutrient-rich, warm, permafrost-free, south-facing slopes, to black spruce forests on poorly drained, nutrient-poor, permafrost soils of north-facing slopes, lowlands, and lower slopes. Standing aboveground tree biomass ranges from 92 to 183 tons/ha for the hardwood stands up to 249 tons/ha for white spruce stands, and 2-11 tons/ha for black spruce stands. Floodplain forests vary from productive stands of balsam poplar and white spruce forming on river alluvium, permafrost-free soils, to slow-growing black spruce and bogs occupying older terraces underlained by permafrost. Young stages of revegetation are dominated by alder and willow shrubs. Aboveground tree biomass ranges from 40-180 tons/ha for balsam poplar stands to 60-245 tons/ha for white spruce stands.

The climate at BCEF is continental, with large diurnal temperature variations, low precipitation, cloud cover and humidity [8]. Mean annual temperature is -3.5°C. Temperature extremes range from +35°C in June to -65°C in January. The annual mean precipitation is 286 mm, with 30% falling as snow.

2. Airborne SAR data and ground truth data

AIRSAR [9] imaged BCEF on March 13, 17 and 19 of 1988 when the forest changed from frozen (March 11) to thawed conditions (March 13) and back to frozen conditions (March 17) due to a transition to unusually warm air-temperatures for the season [10]. On May 4, 6 and 7 of 1991, AIRSAR overflew the study site when the forest changed from flooded (May 4) to unflooded conditions (May 6-7) with the formation and subsequent disappearance of ice jams in the Tanana river. AIRSAR overflew again BCEF in July 1993 when the forest had a fully developed canopy under dry climatic conditions. Data calibration was performed in a similar fashion for all data takes using the radar response from 1.8 m trihedral corner reflectors deployed in clear-cut areas prior to the SAR overflight. The multidate SAR were subsequently co-registered to a SPOT scene.

Between 1988 and 1993, 21 forest stands were inventoried for tree density, DBH, height, canopy depth, and species [11]. Whole-tree aboveground biomass was estimated for each tree from the basic DBH, height, density, and species measurements using empirical, allometric equations [12-14].

3. Results

Radar backscatter values, σ^o, extracted from each stand at each frequency and polarization, and averaged together over the whole stand, are plotted as a function of biomass in Fig. 1. As σ^o eventually approaches a saturation level at the high biomass levels, third order polynomials were fit to the data instead of straight lines. At C-band, σ^o_{HV} saturates at a biomass level less than 50 tons/ha, and σ^o_{HH} and σ^o_{VV} show little sensitivity to aboveground biomass for the forest. This trend is consistent with past observations of other forest types as well as modeling studies [1-5]. C-band radar signals do not penetrate much inside the forest canopy and are mainly scattered by the foliage and branches and twigs of the upper canopy. Hence, σ^o quickly saturates as biomass increases. At the same time, C-band signals are sensitive to differences in canopy structure and separate in fact very well different forest types [15].

At L-band, σ^o is better correlated with forest biomass than at C-band. L-band signals are expected to penetrate deeper inside the canopy and to be scattered mostly by larger branches and the trunk, the biomass of which is correlated to total biomass. The dynamic range of σ^o_{HV} between 5 and 200 tons/ha is 4 dB greater than that measured at C-band, and saturation occurs at about 100 tons/ha. The sensitivity to biomass is less for σ^o_{HH} and σ^o_{VV}.

At P-band, the dynamic range in σ^o_{HV} between 5 and 200 tons/ha is the same as that measured at L-band, but the dynamic range in σ^o_{HH} is increased, and saturation occurs at about 200 tons/ha. P-band H-polarized signals penetrate deeper inside the tree canopy and

0-7803-1497-2/94 $4.00 © 1994 IEEE

may undergo double reflections from the tree-trunks to the forest floor and back to the radar direction. The magnitude of this interaction increases with tree height and must be significant at high biomass levels compared to the volume scattering from the branches [3]. At V-polarization the radar signals are more attenuated during propagation through the trunks, trunk-ground interactions are weaker, yielding $\sigma^o_{VV} < \sigma^o_{HH}$. In contrast, $\sigma^o_{VV} > \sigma^o_{HH}$ in alder or black spruce stands of lower biomass level because trunk-ground interactions are weak for those short trees and direct scattering from the wet understory vegetation and ground layers is significant. Also at P-band, data dispersion associated with difference in forest type is lower than at L-band (for instance for alder and black spruce stands).

4. Radar estimates of aboveground biomass

We derived regression curves relating the logarithm of biomass to third order polynomials in the logarithm of σ^o_{HV}, σ^o_{HH}, or σ^o_{VV} at one frequency. Biomass is then predicted from the radar measurements and compared to inventory estimates (Fig. 2). Here, the effect of the incidence angle θ_i is ignored in the analysis because most stands are imaged at $35^o < \theta_i < 45^o$ for which σ^o is expected to vary by less than $\pm 1\ dB$. At L-band, data dispersion is large above 100 tons/ha (Fig. 2a). Below that level, radar predictions are reasonably accurate but the number of data points is small. For alder stands, the predicted biomass is too high. When a single regression curve is used for all tree species, L-band signals probably are limited to the discrimination of 5 biomass levels: 1) no biomass, 2) less than 5 tons/ha, 3) between 5 and 50 tons/ha, 4) 50 to 100 tons/ha, and 5) above 100 tons/ha, thereby separating, respectively, open water from clear-cuts, black spruce stands, stands of intermediate biomass, and the mature stands of white spruce and balsam poplar. Further studies with more data points are needed to determine whether L-band data could separate additional biomass levels using tree species dependent regression curves.

Radar predictions at P-band HV are more accurate than at L-band HV and extend over almost the entire range of biomass level for these forests (Fig. 2b). σ^o_{HV} separates an additional biomass level between 100 and 200 tons/ha. Adding σ^o_{HH} and σ^o_{VV} to the regression improves the results obtained using only σ^o_{HV} for alder stands (Fig. 2c) because the contrast between σ^o_{HH} and σ^o_{VV} is small and consistent with a low biomass level for these stands. The average absolute difference between predicted biomass and actual biomass at P-band (Fig. 2c) is 29%. If we consider the following 7 biomass levels: 1) 0 to 1 tons/ha; 2) 1 to 4.5 tons/ha; 3) 4.5 to 13 tons/ha; 4) 13 to 45.5 tons/ha; 5) 45.5 to 100 tons/ha; 6) 100 to 178 tons/ha; and 7) > 178 tons/ha, P-band signals predict the biomass levels of the 24 stands with a 18% error rate. In the remaining 4 forest stands predicted biomass values are too high, but 3 of these stands exhibit particular conditions: BP6 is close to the river bank and may have still been partially flooded on May 6, yielding a stronger than expected radar response; BP14 is a very heterogeneous stand (79% standard deviation in biomass) where large uncertainties in predicted biomass level are expected; and WSBP2 exhibit higher than usual σ^o values because balsam poplar trees in that stand are rotten with tree-trunks filled up with water.

For comparison, a similar regression performed on the radar data collected over the Landes forest, France [1] shows little data spread, an average difference between predicted biomass and actual biomass of only 11.2 %, and an error rate of 7% for separating the same biomass levels as above (Fig. 2d). It was understood that in natural forest ecosystems the accuracy of the inversion will be less because tree density, height, diameter and age as well as canopy structure have large spatial variations. At the Landes site, stand biomass is known with 12.5% accuracy and stands are more or less uniform. At BCEF, standard deviation in biomass within each stand is 34% of the stand biomass in average, up to 79% for BP14. Tree height, density, and height commonly vary by more than one order of magnitude from one plot to the next or even within the same plot; and the radar signals interact with a canopy of spatially varying three-dimensional structure because the forest stands include tree gaps, old river sloughs, and mixtures of different species at various ages.

6. Other results

The radar response from the forest changed by as much as 6 dB between spring and winter/frozen, which is as much as the sensitivity of σ^o_{HV} to stand biomass [10]. Hence, an inversion curve derived from winter data would not yield reliable estimates of biomass at another season. In interior Alaska, where environmental conditions vary dramatically during a seasonal cycle, it is expected that radar mapping of aboveground dry biomass will be season and environmental conditions dependent. At the same time, the temporal variability of σ^o may provide additional information about the forest such as the water status of the soil and vegetation, or foliage biomass.

On May 6, 1991, AIRSAR imaged BCEF at 4 different look angles: $\theta = 23^o, 30^o, 40^o$, and 50^o. L-band data were calibrated to within 1-2 dB based on the radar response from 1.8m trihedral reflectors. Data calibration could not be performed as accurately at P-band at the smaller look angles because the size and orientation of the corner reflectors were no longer optimal at that frequency and look angle; therefore only the L-band results are shown in Fig. 3. Between 25^o and 50^o, σ^o_{HV} varies by less than 1 dB compared to 3-4 dB for σ^o_{HH}. A smaller dependence of σ^o_{HV} with the incidence angle θ_i is expected because the radar returns are dominated by volume scattering from tree branches which is less dependent on θ_i. At H-polarization, modeling studies predict that scattering from trunk-ground interactions is quite sensitive to θ_i [3]. When $\theta_i < 25^o$ or $\theta_i > 50^o$, however, σ^o_{HV} differs significantly from its average level at 30-50^o. At those high and low angles, the radar will respectively underestimate and overestimate biomass if θ_i is ignored in the inversion. We verified this effect of θ_i for 3 south-facing upland stands which were facing away from the radar on May 6, 1991. These stands have a stand biomass of 103, 24, and 92 tons/ha, respectively, and were imaged at $\theta_i = 53^o, 61^o$, and 58^o. Their predicted biomass level is 42, 4, and 16 tons/ha, clearly several orders of magnitude lower than the actual values. Hence, topographic information is required for reliable mapping of aboveground biomass in these areas.

7. Conclusions

This study suggest SARs operating at long radar wavelengths have potential for mapping aboveground biomass of boreal forests in interior Alaska, a variable of prime importance to carbon cycling investigations, ecosystem studies and forest management applications. At P-band, predicted biomass values from the radar are 29 % in error in average but the radar discriminates 7 biomass levels with 82% accuracy over 24 forest stands. It was understood that data dispersion would be more significant for natural forest ecosystems than for forest plantations because uncertainties in estimating aboveground biomass in natural forests are large due to spatial variations in tree species, age, density, height, and DBH, and also due to complex interactions of the radar signals with a spatially varying three-dimensional structure of the canopy. Also changing environmental conditions have a pronounced effect on radar backscatter from the forest, especially in Alaska, so inference of biomass from the radar data depends on the environmental state of the forest. Finally, radar data must be combined with topographic maps to obtain reliable radar estimates of forest biomass in areas of significant topography.

ACKNOWLEDGEMENTS This work was carried out at the Jet Propulsion Laboratory, California Institute of Technology, under contract with the National Aeronautics and Space Administration.

REFERENCES

[1] LeToan T., A. Beaudoin, J. Riom, D. Guyon, Relating forest biomass to SAR data, *IEEE Trans. Geosc. Rem. Sens.* 30, 403-411, 1992.

[2] Dobson M. C., F. T. Ulaby, T. LeToan, A. Beaudoin, E. S. Kasischke, and N. Christensen, Dependence of radar backscatter on conifer forest biomass,

IEEE Trans. Geosc. Rem. Sens. **30**, 412-415, 1992.

[3] van Zyl J. J., The effect of topography on radar scattering from vegetated areas, *IEEE Trans. Geosc. Rem. Sens.* **31**, 153-160, 1993.

[4] Beaudoin A. and 9 others, Retrieval of forest biomass from SAR data, *Int. J. Rem. Sens.*, Sept. 1994, In Press.

[5] Mc Donald K., M. C. Dobson, and F. T. Ulaby, Using MIMICS to model multiangle and multitemporal backscatter from a walnut orchard, *IEEE Trans. Geosc. Rem. Sens.* **28** 477-491, 1990.

[6] van Cleve K., L. Oliver, R. Schlentner, L. A. Viereck, and C. T. Dyrness, Productivity and nutrient cycling in taiga forest ecosystems, *Can. J. For. Res.* **13**, 747-766, 1983.

[7] Viereck, L.A., van Cleve, K., and Dyrness, C. T., Forest ecosystem distribution in the taiga environment, In *Ecol. Ser. Vol. 57, For. Ecos. in the Alaskan Taiga* (Van Cleve, K. Ed.), Springer-Verlag, NY, pp 22-43, 1986.

[8] Slaughter, C.W., and Viereck, L.A., Climatic characteristics of the taiga in interior Alaska, In *Ecol. Ser. Vol. 57, For. Ecos. in the Alaskan Taiga* (Van Cleve, K., Ed.), Springer-Verlag, NY, pp 2-21, 1986.

[9] van Zyl J. J., R. Carande, Y. Lou, T. Miller, and K. Wheeler, The NASA/JPL three-frequency polarimetric AIRSAR system, *Proc. Int. Geosc. Rem. Sens. Symp.*, Houston, Texas, May 26-29, 1992, IEEE NY Pub., 649-651, 1992.

[10] Way, J. B. and 15 others, The effect of changing environmental conditions on microwave signatures of forest ecosystems: preliminary results of the March 1988 Alaskan aircraft SAR experiment, *Int. J. Rem. Sens.* **11**, 1119-1144, 1990.

[11] Rignot E., J.B. Way, C. Williams, L. Viereck, J. Yarie, T. LeToan, Radar estimates of aboveground biomass in boreal forests of interior alaska, *IEEE Trans. Geosc. Rem. Sens.*, Sept., 1994.

[12] Manning G. H., M. R. G. Massie, and J. Rudd, Metric single-tree weight table for the Yukon territory, Information Rept. BX-X-250. Can. For. Serv., Pacific Forest Research Centre, Victoria, B.C. 60 pp., 1984

[13] Singh T., Weight tables for important tree species in the Northwest territories. Forest management note N. 27, Can. For. Serv., Northern Forest Research Centre, Edmonton, Albera, 4 pp., plus tables, 1983.

[14] Yarie J, and K. van Cleve, Biomass and productivity of white spruce stands in interior Alaska. *Can. J. For. Res.* **13**, 767-772, 1983.

[15] Rignot E., C. William, J. B. Way, and L. Viereck, Mapping of forest types in Alaskan Boreal forests using SAR imagery, *IEEE Trans. Geosc. Rem. Sens.*, Sept., 1994.

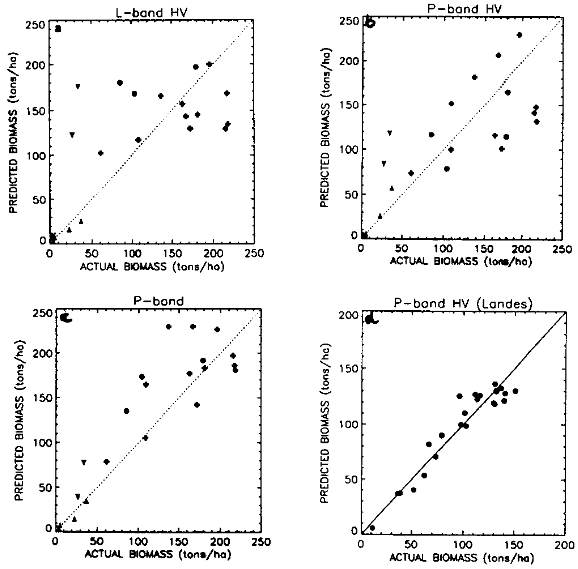

Figure 2. Predicted biomass levels of various forest stands from BCEF versus actual biomass levels at (a) L-band HV-polarization; (b) P-band HV-polarization; and (c) P-band HH-, HV-, and VV-polarizations. Predicted biomass levels for the Landes forest, France at (d) P-band HV-polarization.

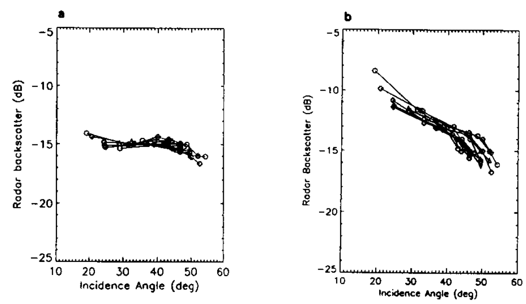

Figure 3. σ^o values of various forest stands versus the incidence angle of the radar illumination for multiple incidence angle SAR data acquired on May 6, 1991 at L-band frequency (a) HV-polarization; and (b) HH-polarization. Continous lines connect data points obtained from the same forest stand imaged at different look angles. A constant offset factor has been applied on each line (a different constant factor for each stands) to facilitate inter-stand comparison of the dependence of σ^o on the incidence angle, regardless of the absolute level in radar backscatter of each stand. Symbols for various forest stands are the same as in Fig. 1.

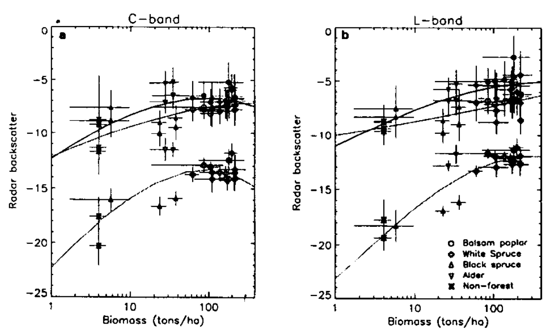

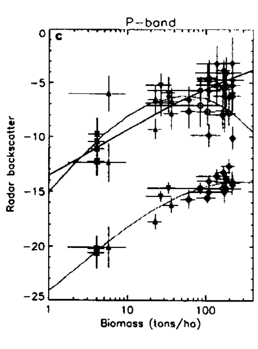

Figure 1. Radar backscatter σ^o (in dB) at HH- (black dots), HV- (grey dots), and VV-(white dots) polarization (H means horizontal and V means vertical) of 21 forest stands versus whole-tree above-ground dry biomass (in tons/ha) in log-log scale at (a) C-band; (b) L-band; (c) P-band on May 6, 1991. Thin horizontal and vertical bars correspond, respectively, to the standard deviations in biomass and σ^o for each forest stand. Continous lines are from third-order polynomial regressions relating σ^o in dB to the logarithm of the stand biomass.